Dynamic k_T-points: a new concept to improve T_2-weighted imaging at 7T

Florent Eggenschwiler[1], Kieran R. O'Brien[2,3], Bénédicte Maréchal[3,4], Rolf Gruetter[1,2], and José P. Marques[5]

[1]*Laboratory for Functional and Metabolic Imaging, Ecole Polytechnique Fédérale de Lausanne, Lausanne, Vaud, Switzerland,* [2]*Department of Radiology, University of Geneva, Geneva, Geneva, Switzerland,* [3]*CIBM - AIT, École Polytechnique Fédérale de Lausanne, Lausanne, Vaud, Switzerland,* [4]*Advanced Clinical Imaging Technology, Siemens H IM BM PI, Lausanne, Vaud, Switzerland,* [5]*Department of Radiology, University of Lausanne, Lausanne, Vaud, Switzerland*

Introduction:

T_2-weighted images are widely used for the diagnosis of brain diseases involving gray- and white-matter lesions such as multiple sclerosis. The increased SNR available at high field strengths (≥3T) should provide higher spatial resolution; however, the inhomogeneous distribution of the RF field (B_1^+) causes undesirable signal and contrast variations of GM/WM across the brain. In a previous study[1], high quality whole brain T_2-weighted imaging was achieved by combining short 3D tailored RF pulses (k_T-points[2]) with a variable flip angle TSE (SPACE[3]) sequence. A single k_T-point pulse was designed in the STA regime to replace all the sequence pulses (here referred to as **static k_T-point design**). In this work, a specific k_T-point pulse is designed for each pulse of the sequence (**dynamic k_T-point design**) in order to further improve T_2-weighted imaging homogeneity.

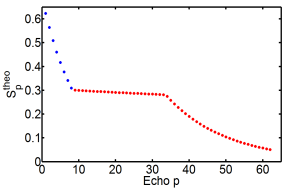

Fig. 1: Signal at each echo of the TSE sequence simulated for the described protocol and assuming no B_1^+ inhomogeneity. Blue and red points correspond to echoes in the initial ramp and static pseudo-steady state, respectively.

Methods:

Two healthy subjects, who provided informed consent, were scanned on a MAGNETOM 7T scanner (Siemens AG Healthcare Sector, Erlangen, Germany) equipped with a 32-channel receive head coil (NOVA Medical, USA). Protocols:

B_1^+ map – SA2RAGE[4] sequence: TR/TD_1/TD_2 = 2.4/0.0054/1.8s, res. = 3.4x3.4x4.0mm^3, matrix = 64x64x48, T_{acq} = 1min55s.

TSE sequence: TR/TE = 2s/100ms, echo train length (ETL)/echo spacing (ES) = 57/4.16ms, RF_{Dur} = 1.40ms, res. = 0.85x0.85x0.85mm^3, matrix = 256x256x176, iPAT = 3, T_{acq} = 6min30s.

The k-space trajectory defining the k_T-point positions was determined by designing a first k_T-point pulse in the STA regime using the SOLO algorithm[5] fed with the subject-specific B_1^+ profile. This first estimation was used as a starting point for subsequent optimizations. The k-space trajectory was maintained throughout the entire sequence.

The Spatially Resolved Extended Phase Graph (SR-EPG) formalism[6] including k_T-point pulses was used to simulate the signal across the TSE sequence. When considering a sequence of ETL pulses made of N k_T-points each, the goal is to optimize the amplitude $A_{i,j}$ and phase $\varphi_{i,j}$ of each sub-pulse of the k_T-points i (i=1-N) and RF pulses j (j=0-ETL) in order to make the signal throughout the sample $S_p(\mathbf{r})$ as close as possible to the expected signal S_p^{theo} (cf. Fig. 1) for all echoes across the sequence (dynamic k_T-point design).

The optimization problem was split into two parts: initial ramp – transition towards static pseudo-steady state[7] (blue part in Fig. 1) and maintenance of signal homogeneity throughout echoes in pseudo-steady state (red part in Fig. 1).

For the initial ramp, the amplitudes $A_{i,j}$ and phases $\varphi_{i,j}$ (with j=0-10) were optimized simultaneously using a gradient descent algorithm[8] using a magnitude least squares (MLS) cost function. The second part of the sequence was optimized on a k_T-point pulse-by-k_T-point pulse basis. For each pulse optimization, the amplitudes and phases of the previously optimized k_T-point pulse are used as an initial guess. To reduce computation time, optimizations were performed on voxels belonging to a subject-specific brain mask calculated using a homebuilt software.

The SR-EPG framework was subsequently used to simulate the signal throughout the TSE train for: (1) standard hard pulses; (2) static k_T-point pulses; (3) dynamic k_T-point pulses. The quality of each approach was evaluated in terms of signal fidelity ($\| |S_p(\mathbf{r})|-|S_p^{theo}| \|$ for each echo) and signal homogeneity (standard deviation throughout each simulated $S_p(\mathbf{r})$ map). In (2) and (3), 3 and 5 k_T-points were used for each sequence pulse.

To support simulations, TSE images acquired with k_T-point pulses designed statically and dynamically were compared with images acquired with standard hard pulses (no k_T-point).

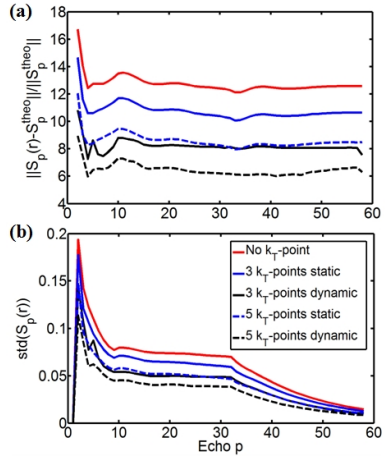

Fig. 2: (a) Deviations between sequence echoes and theoretical signal (Fig. 1). (b) Standard deviation across each echo map $S_p(\mathbf{r})$ for the different RF pulse designs.

Results and discussion:

The curves presented in Fig. 2a and 2b show the improvement provided by the dynamic k_T-points over the static k_T-point design and the approach without k_T-point in terms of both echo train fidelity and homogeneity. It can be seen that the solution resulting from the use of 3 dynamic k_T-points is comparable to the one obtained with 5 k_T-points in the static regime. Moreover, for the same RF duration, the sequence designed with 3 dynamic k_T-points outperformed the one with 5 static k_T-points by more than 50% in terms of SAR. Despite the increased homogeneity obtained using a higher number of k_T-points, measured images were acquired using 3 k_T-points to keep the RF duration shorter than 1.5ms within the SAR limits.

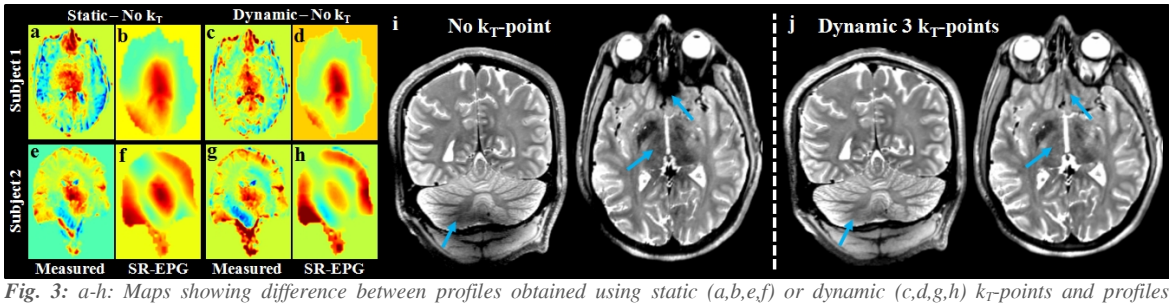

Fig. 3: a-h: Maps showing difference between profiles obtained using static (a,b,e,f) or dynamic (c,d,g,h) k_T-points and profiles obtained with hard pulses, experimentally measured (a,c,e,g) and calculated via SR-EPG simulations (b,d,f,h). a-d maps are associated to subject n°1 and e-h maps to subject n°2. i-j: TSE images acquired without (i) and with dynamic 3 k_T-point pulses (j) for subject n°1. Blue arrows highlight brain regions with noticeable improvements.

The differences "static - no k_T-point" and "dynamic - no k_T-point" calculated for the measured TSE images (Fig. 3 a,c,e,g) are in close agreement with the ones simulated using the SR-EPG at k-space center (Fig. 3 b,d,f,h) for both subjects. This shows that the state of the magnetization throughout the TSE sequence can be reliably understood with SR-EPG simulations including static and dynamic k_T-points. TSE images acquired without and with dynamic k_T-points are shown in Fig. 3 i-j. High improvements in signal and contrast homogeneity are seen in the cerebellum, brain center and over sinuses (blue arrows) when using dynamic k_T-points.

Conclusion:

The very good agreement between simulations and experimental data demonstrates that including k_T-points in the SR-EPG formalism provides a new degree of freedom to control the magnetization distribution in a TSE sequence with variable flip angles leading to T_2-weighted images with high level of signal and contrast homogeneity at 7T. This methodology will now be translated to parallel transmission where the advantages are expected to be greater thanks to the increased number of degrees of freedom associated with the different transmit channels.

References: [1] Eggenschwiler et al, MRM, in press, 2013, [2] Cloos et al, MRM 67, 2012, [3] Mugler et al, ISMRM, 2001, p.438, [4] Eggenschwiler et al, MRM 67, 2012, [5] Ma et al, MRM 65, 2011, [6] Malik et al, MRM 68, 2012, [7] Alsop et al, MRM 37, 1997, [8] Avriel, Nonlinear Programming: Analysis and Methods, Dover Publishing, 2003.

Acknowledgements: Supported by the CIBM of the UNIL, UNIGE, HUG, CHUV, EPFL and the Leenaards and Jeantet Foundations.